Chemistry–A European Journal
Research Article
doi.org/10.1002/chem.202300771
Chemistry Europe
European Chemical Societies Publishing
www.chemeurj.org

Azide-Substituted 1,2,3-Triazolium Salts as Useful Synthetic Synthons: Access to Triazenyl Radicals and Staudinger Type Reactivity

Felix Stein,[a, b] Simon Suhr,[b] Arijit Singha Hazari,[b] Robert Walter,[b] Maite Nößler,[a] and Biprajit Sarkar*[b]

Abstract: Mesoionic carbenes (MIC) are a popular class of compound that are heavily investigated at the moment. The access to cationic MICs, and the ability of MICs to stabilize radicals are two highly attractive fields that have hardly been explored until now. Here the synthesis and characterisation of three different cationic azide-substituted 1,2,3-triazolium salts, used as building blocks for studying their reactivity towards triphenylphosphine are reported, where the reactivity is dependent on the nature of the starting triazolium salt. Furthermore, the cationic triazolium salts were used to develop a series of unsymmetrical MIC-triazene-NHC/MIC' compounds, which can be readily converted to the radical form either by electrochemical or chemical methods. These radicals, which display NIR electrochromism, were investigated using a battery of techniques such as electrochemistry, UV/Vis/NIR and EPR spectroelectrochemistry, and theoretical calculations. Interestingly, the MIC plays an important role in the stabilization of the triazenyl radical, particularly in a competitive role vis-à-vis their NHC counterparts. These results shed new light on the ability of MICs to stabilize radicals, and possibly also on their π-accepting ability.

Introduction

Since the discovery of the first organic azide,[1] namely phenyl azide in 1864, this small and energy-rich class of compound has been used in a wide variety of transformations and different substitution patterns are possible:[2] (a) formation of nitrene via loss of N_2;[3] (b) reaction with an electrophile at the substituted nitrogen (N^1);[4] (c) reaction at the terminal (N^3) with a nucleophile[5,6] and (d) cycloaddition with a dipolarophile.[7] With the introduction of N-*heterocyclic* carbenes (NHC) as the substituent, the stability of the azide is enhanced by steric bulk and good π-acceptor properties.[8] These azido-azolium salts are well established and described in the literature.[9] Several examples are known where such azido-azolium salts are used for the synthesis of triazenyl compounds,[10–14] aziridines with diverse substituents,[15] for diazo-transfer to primary amines,[16] or in a Staudinger type reaction leading to the formation of iminophosphoranes.[10] Recently, E. Lee and co-workers synthesized a variety of different unsymmetrical NHC substituted triazenyl compounds, which can be used as anolytes for non-aqueous organic redox flow batteries.[13] Furthermore, they could show that triazenyl radicals can be stabilized by two symmetrical NHC flanking units, due to the their enhanced π-acceptor ability, which results in a delocalisation of the spin density onto the carbene moiety.[12]

This is a rare example of nitrogen-centred radicals, which are stabilised by NHCs. The stabilization of radicals by using carbenes such as NHCs and CAACs is a very vibrant field of research.[17,18] Despite the progress in synthetic chemistry, the stability imparted by carbenes to radicals is not yet fully understood. To overcome this problem, Munz and co-workers investigated the stabilization of radicals by a frontier orbital picture.[19] They were able to show that both the π-acceptor and the π-donor abilities of the substituents are important for the stabilisation. Also, a small HOMO–LUMO gap is beneficial for a good stabilisation of the radical. In contrast to NHCs, mesoionic carbenes (MIC) benefit from their high-lying HOMO levels, which makes them better donors, and also generates a smaller HOMO–LUMO gap in them.[20,21] Interestingly, the research field of MIC adducts of group 15 elements is largely underexplored. Only a few examples with nitrous oxide and diaza compounds were reported by Severin and co-workers.[22,18] MICs, particularly of the triazolylidene type, have been reported to be poor π-acceptors, and thus their ability to stabilize radicals have hardly been explored. Recently, we and others have shown that it is indeed possible to stabilize radicals based on such MICs.[23–25]

[a] F. Stein, M. Nößler
Institut für Chemie und Biochemie, Anorganische Chemie
Freie Universität Berlin
Fabeckstraße 34–36, 14195, Berlin (Germany)

[b] F. Stein, S. Suhr, Dr. A. Singha Hazari, R. Walter, Prof. Dr. B. Sarkar
Institut für Anorganische Chemie
Universität Stuttgart
Pfaffenwaldring 55, 70569 Stuttgart (Germany)
E-mail: biprajit.sarkar@iac.uni-stuttgart.de
Homepage: http://www.iac.uni-stuttgart.de/en/research/aksarkar/

Supporting information for this article is available on the WWW under https://doi.org/10.1002/chem.202300771

A very powerful synthetic synthon to access much of the interesting chemistry mentioned above and beyond will be azide-substituted 1,2,3-triazolium salts, which will be useful building blocks for a variety of reactions (Scheme 1). Synthetic access to such building blocks which could potentially generate cationic MICs remain very rare, and the few that are known display excellent follow-up chemistry.[20,26] In the following, we present first reports on azide-substituted 1,2,3-triazolium salts. We show that after photochemical or thermal activation, the azido-triazolium salt reacts with triphenylphosphine following a Staudinger type reaction protocol. Furthermore, a series of redox-active triazenyl compounds, supported by mixed MIC and NHC flanking units are synthesized and crystallographic characterized. We investigated the spectroscopic properties of these complexes with a combination of different methods like cyclic voltammetry, UV/Vis/NIR and EPR spectroelectrochemistry as well as with theoretical methods. To the best of our knowledge, this work represents the first report of a MIC-triazenyl based radical, in which the MIC unit plays a crucial role in the stabilisation of the radical.

Results and Discussion

Synthesis, Characterisation, and Reactivity

The complete synthetic procedure for the synthesis of the azide-substituted 1,2,3-triazolium salts is reported in Scheme S1. In total, 3 different synthetic routes were utilized to obtain the cationic mono azido-triazolium salt (**L1**), the diazido-substituted-bis-triazolium salt (**L2**) and the methylene bridged diazido-substituted-bis-triazolium salt (**L3**, Scheme 2). Whereas for **L1** and **L2** the 1,5 regioisomer of the corresponding triazole was used, the 1,4 regioisomer of the triazole was used for **L2**. The starting point of all three compounds is a chloro-substituted triazole (**1** and **2**), which is generated by deprotonation of the corresponding triazole, followed by a chlorination with hexachloroethane as a chlorinating agent. After alkylation, the corresponding triazolium salts were obtained in good yields (70% to 89%). While Meerwein salt served as an alkylating agent in the synthesis of **2** and **5**, freshly prepared bis(trifluormethanesulfonate)methane was used to generate the methylene-bridged species **6**. To obtain the azide-substituted triazolium salts, all three aforementioned triazolium salts were reacted with sodium azide under the exclusion of light in dry DCM for 4 days, as light apparently induces decomposition of the desired products. After purification, all compounds could be obtained in moderate to good yields between 70% and 81%.

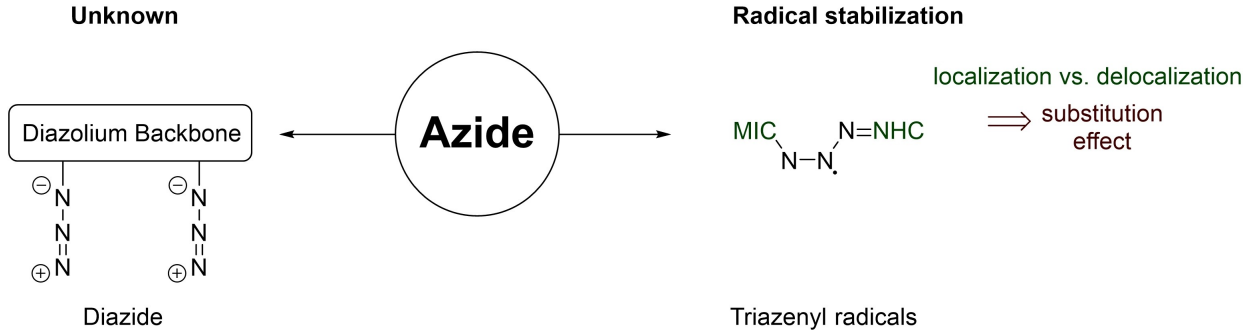

Scheme 1. Schematic representation of the application of substituted azides.

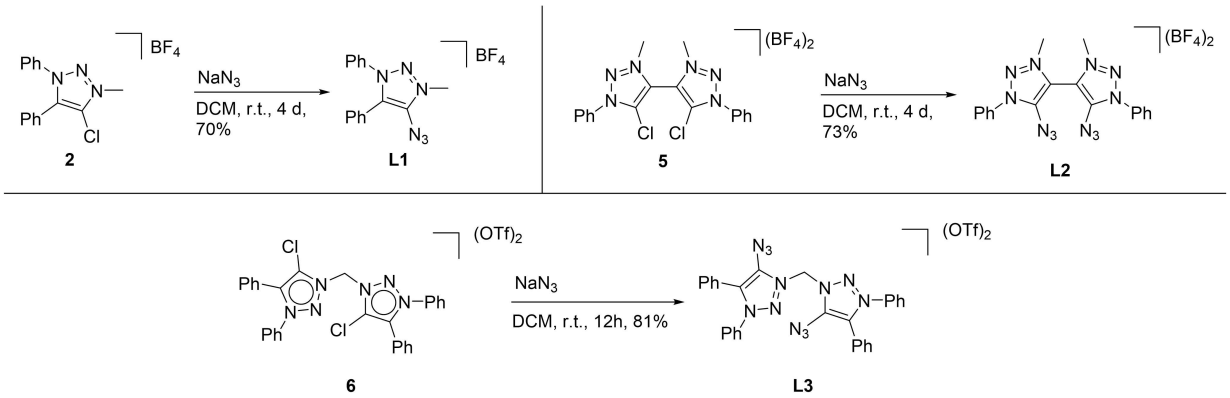

Scheme 2. Synthesis of azido-triazolium salts.

The compounds were characterized by NMR spectroscopy, IR-spectroscopy, and mass spectrometry.

It was also possible to grow crystals for several of the chloro-substituted compounds as well as the cationic azido-triazolium salts described above, that were suitable for X-ray diffraction measurements (Figure 1, see Supporting Information, Figure S26–S34). In the following section, only structural properties of the azide containing compounds are discussed. While **L2** crystalises in the triclinic P −1 space group, **L1** and **L3** crystallizes in the monoclinic P 1 21/c 1 space group respectively (Table S13). The angle between the three nitrogen atoms of the azide were observed to be in between 170.7(7)° and 171.8(1)°, which is a bit more bent than the comparable azido-imidazolium salt described in the literature.[23] The bond length of N4-N5 and N5-N6 ranges between 1.254 Å–1.259 Å and 1.129 Å–1.130 Å (Table 1), which is in good agreement with the literature reported values.[10,27] Furthermore, the N–N and C–N bond lengths within the triazolium rings were also observed to be in the expected range and point to a delocalized bonding situation in the heterocyclic rings.

The electronic structures of the azido-triazolium salts were probed via IR spectroscopy. Indeed, an intense characteristic band was observed between 2153 cm^{-1} and 2155 cm^{-1} for all three compounds (Figure S31), which is in accordance with values reported for related azide containing compounds in the literature.[28,16,15]

To investigate their reactivity, the cationic azido-triazolium salts reacted with triphenylphosphine (PPh_3) under irradiation of light or under thermal conditions following a Staudinger type protocol (Scheme 3).[5] In these types of reactions, usually the terminal nitrogen of the azide reacts with triphenylphosphine, resulting in an iminophosphorane after loss of dinitrogen. Indeed, after the reaction of **L1** with 1 equivalent of PPh_3 for 1 h, **MIC-N-PPh$_3$** could be obtained by recrystallisation. This was confirmed by a shift in the ^{31}P NMR singlet resonance to 16 ppm in the downfield region compared to PPh_3, which can be explained by σ-donation from the lone pair of the phosphorus to the nitrogen. The molecular structure of **MIC-N-PPh$_3$** was confirmed by single crystal X-ray diffraction measurements. Crystallographic data revealed a bond length of 1.337(4) Å between the carbene C1 and N4 atoms and a bond angle of 133.5(2)° between C1-N4-P1 which are in accordance with the values reported for the analogous NHC–N-PPh_3 compounds (Figure 2).[10] The electrochemical property of the compound was investigated with cyclic voltammetry and it showed one irreversible reduction process at −2.4 V vs FcH/FcH^+ in DCM (Figure S38). To characterize the intermediate

Table 1. Selected bond lengths (Å) and bond angels (°) for **L1**, **L2**, and **L3**.

	L1	L2	L3
C1-N4	1.358 (5)	1.388 (2)	1.391 (5)
N4-N5	1.256 (6)	1.254 (2)	1.259 (6)
N5-N6	1.130 (9)	1.129 (2)	1.129 (9)
N4-N5-N6	170.7 (7)	171.9 (2)	170.9 (2)

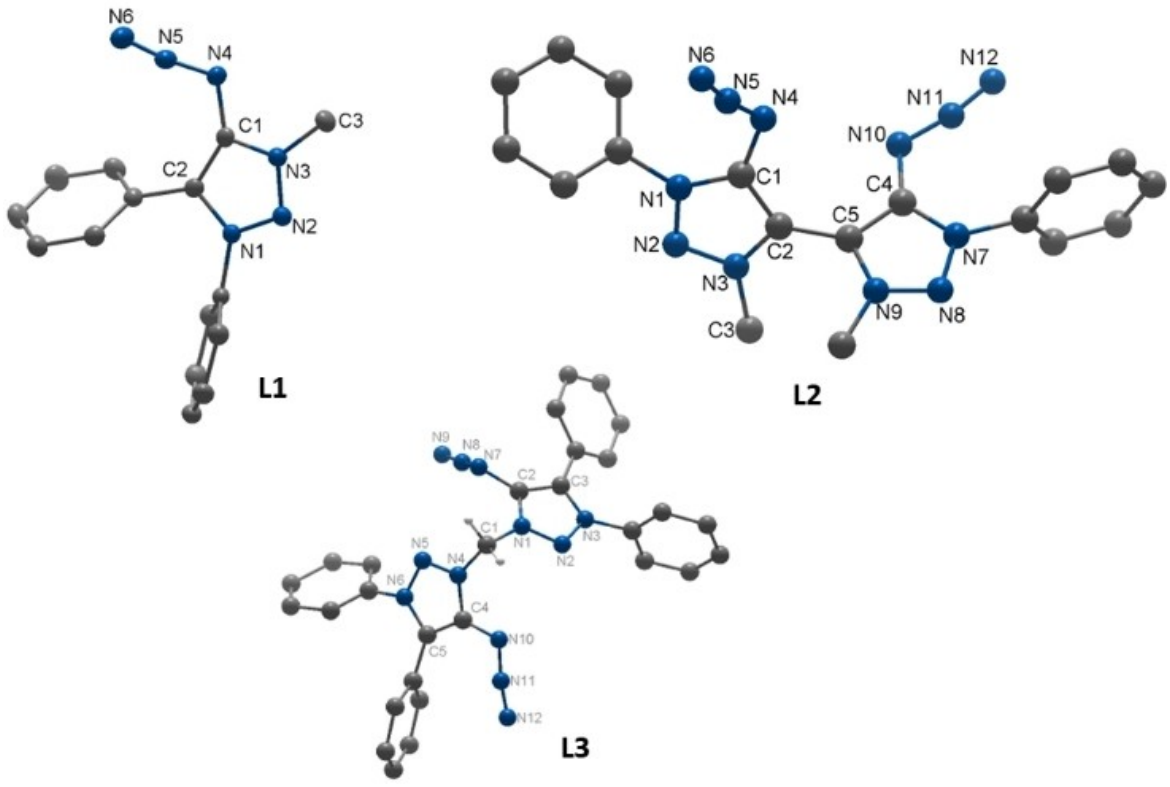

Figure 1. ORTEP representation of **L1**, **L2**, and **L3**: ellipsoids drawn at 50% probability. Solvent molecules, H atoms, and counter anions are omitted for clarity.

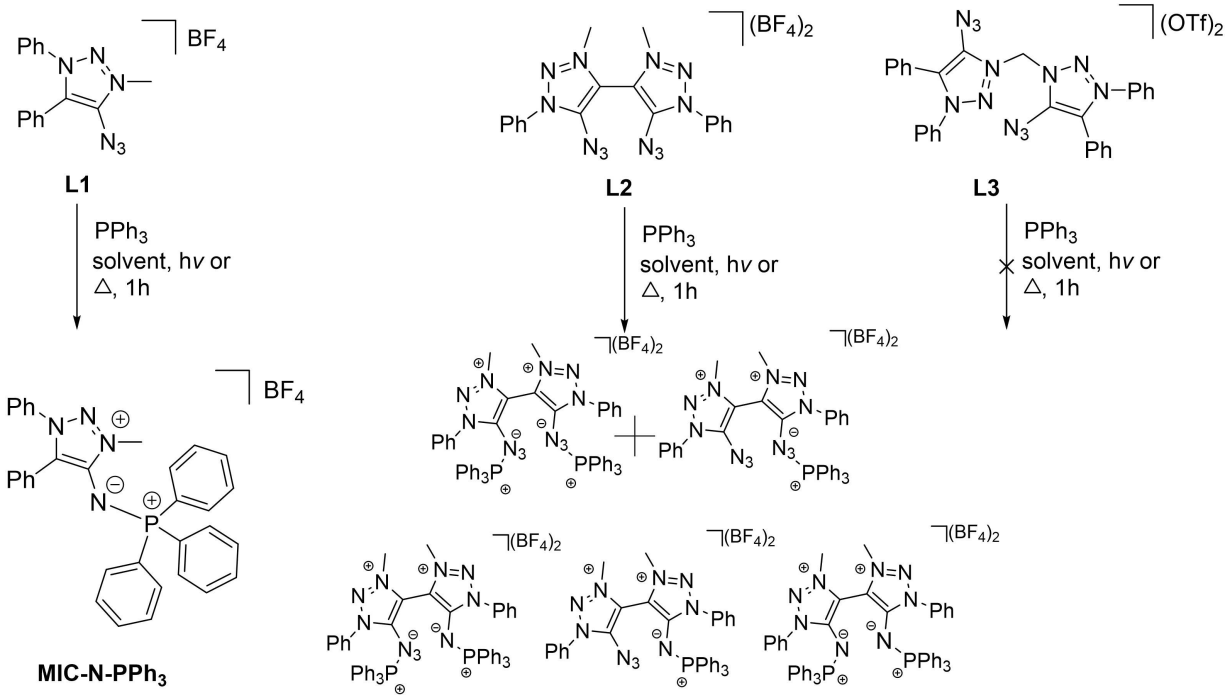

Scheme 3. Reaction of **L1**, **L2** or **L3** with triphenylphosphine under thermal or photochemical conditions.

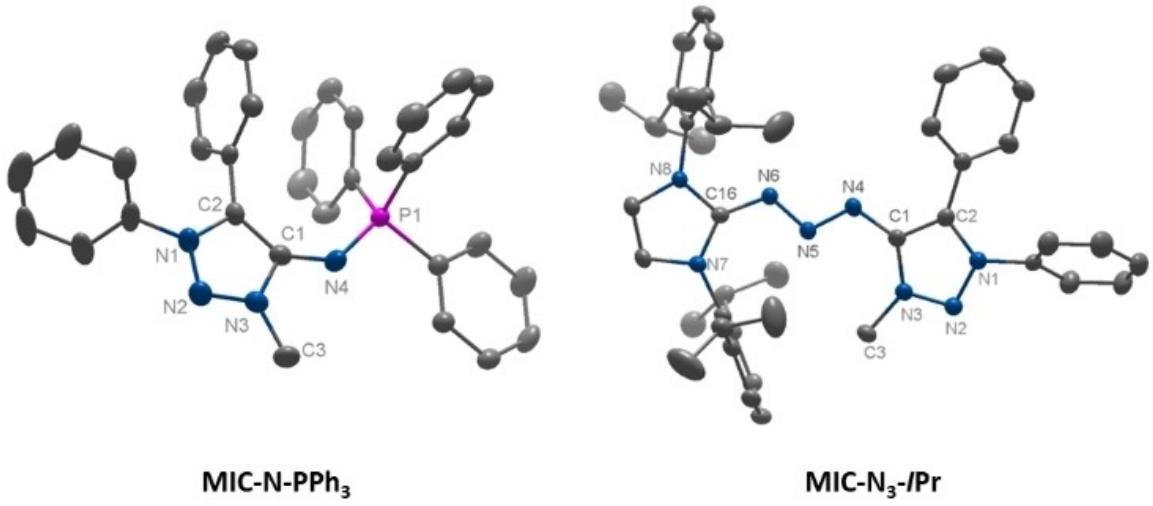

Figure 2. ORTEP representation of **MIC-N-PPh$_3$** (left) and **MIC-N$_3$-*I*Pr** (right): ellipsoids drawn at 50% probability. Solvent molecules, counter anions, and H atoms omitted for clarity.

where the PPh_3 is bound to the azide, the reaction was conducted at 0 °C under exclusion of light. Due to the extremely fast nature of the reaction, a small ^{31}P NMR resonance at 24.58 ppm, attributed to triphenyl phosphine bound to the terminal nitrogen of the azide, can be observed for approximately 1 minute only (Figure S18).

The reaction of **L2** with 2 equivalents of PPh_3 gave a mixture of all possible combinations of the azide and iminophosphorane moieties with PPh_3, as confirmed from mass spectrometry (Scheme 3 and Figure S25). Unfortunately, it was not possible to separate all fractions and even after changing the reaction parameters, no defined and pure product could be obtained. After the reaction of **L3** with 2 equivalents of PPh_3, no distinct product could be observed. A possible explanation for the observation can be the unstable nature of the methylene bridge under the reaction conditions, which was also noted previously by us.[29]

After having achieved the selective and successful reaction of **L1** with PPh_3, we were interested in further exploring the potential of this cationic azido-triazolium unit with a particular

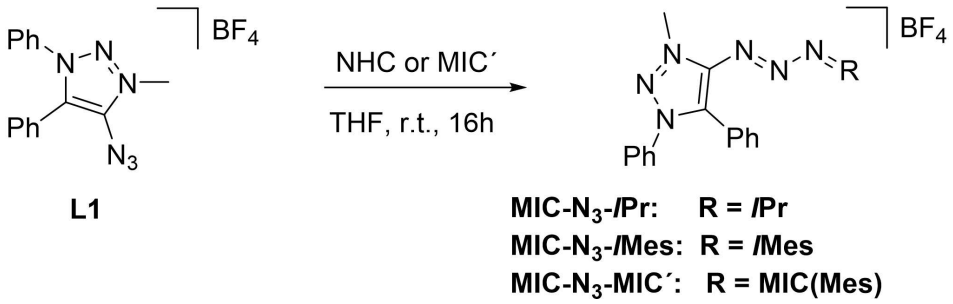

Scheme 4. Synthetic protocol for the synthesis of **MIC-N_3-/Pr**, **MIC-N_3-/Mes**, **MIC-N_3-MIC′**.

focus on generating stable nitrogen-based radicals. While treating **L1** with a variety of free NHCs and one MIC, the terminal nitrogen of the azido-triazolium salt was observed to act as an electrophile with the sterically hindered electron donors (Scheme 4). Following this, a series of unsymmetrical MIC-N_3-NHC/MIC′ compounds were prepared. The NHCs 1,3-Bis(2,4,6-trimethylphenyl)-imidazol-2-ylidene (/Mes) and 1,3-Bis(2,6-diisopropylphenyl)-imidazol-2-ylidene (/Pr) are available in the free form for this reaction (Scheme 4), whereas the mesoionic carbene, 1,4-di-mesityl-3-methyl-1,2,3-triazolylidine (MIC′) was generated in-situ from the corresponding triazolium salt (see Supporting Information). The conversion of **L1** to the desired triazenes was monitored by IR-spectroscopy. The band observed for **L1** at 2155 cm^{-1} disappears after the formation of the triazene (Figure S35 and S36) and can be explained by the coordination of the NHC/MIC′ to the terminal nitrogen of **L1**. While NMR spectroscopy unequivocally confirms the formation of all three triazenes (Scheme 3 and Figure S19–S24), it was also possible to confirm the molecular structure for **MIC-N_3-/Pr** by single crystal X-ray diffraction. The compound contains a W-shaped R′C-N_3-CR″ moiety with bond lengths of 1.292(2) Å and 1.311(2) Å between N4-N5 and N5-N6 (Figure 2), indicating a bond order of 1.5 over the triazene moiety. The experimentally obtained bond parameters were found to be in good agreement with the DFT optimized structures (Table S12). The overall bond lengths and bond angles are in agreement with the comparable unsymmetrical structures reported by Lee and co-workers.[12]

Electrochemistry

The electrochemistry of all three triazenes was first investigated with cyclic voltammetry (Figure 3). In DCM, with NBu_4PF_6 as supporting electrolyte one irreversible oxidation and one reversible one-electron reduction were observed. Comparison of the oxidation potentials revealed peak potential in the range between 1.04 V to 1.27 V at a scan rate of 100 mVs^{-1}. The shape of the oxidation event remained intact with the variation of scan rates. The half-wave potentials for the reduction span a range of 240 mV. The lowest (in terms of absolute value) potential $E_{1/2} = -1.76$ V corresponds to **MIC-N_3-/Mes** followed by $E_{1/2} = -1.90$ V and -2.00 V for **MIC-N_3-/Pr** and **MIC-N_3-MIC′**,

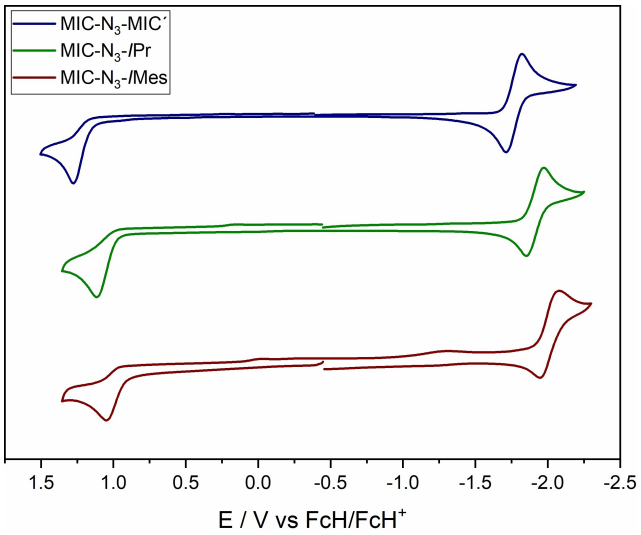

Figure 3. Cyclic voltammograms of the investigated triazenes (scanrate: 0.1 mVs^{1}, in DCM, electrolyte: NBu_4PF_6 (0.1 M), electrode: glassy carbon) under Ar; current normalised.

respectively. The difference in the reduction potential between the two triazenes containing different NHC moieties can be explained by the influence of the substitution pattern on the flanking units of the NHC, and that of the MIC′ containing compound through its stronger donating power.

To further investigate the nature of the reduced species, the compound **MIC-N_3-/Pr** was thoroughly investigated via UV/Vis/NIR spectroelectrochemistry, combined with EPR spectroelectrochemistry (SEC) and theoretical calculations. The UV/Vis/NIR-SEC was performed in DCM in an optically transparent thin layer electrochemical (OTTLE) cell. The initial spectrum showed absorptions in the UV region at 362 nm and 222 nm, typical for this kind of organic molecules.[14] Upon reduction a new band at 410 nm is observed. Surprisingly, a broad band between 1000 nm and 2000 nm with a maximum at 1450 nm and extinction coefficient of 3.76×10^3 $M^{-1}cm^{-1}$ also grew concomitantly (Figure 4). According to the calculations, this can be assigned to a charge transfer band due to the delocalization of the radical between the triazenyl and triazene moiety (see Supporting Information). After reoxidation, the initial spectrum could be recovered, and the broad absorption band in the NIR

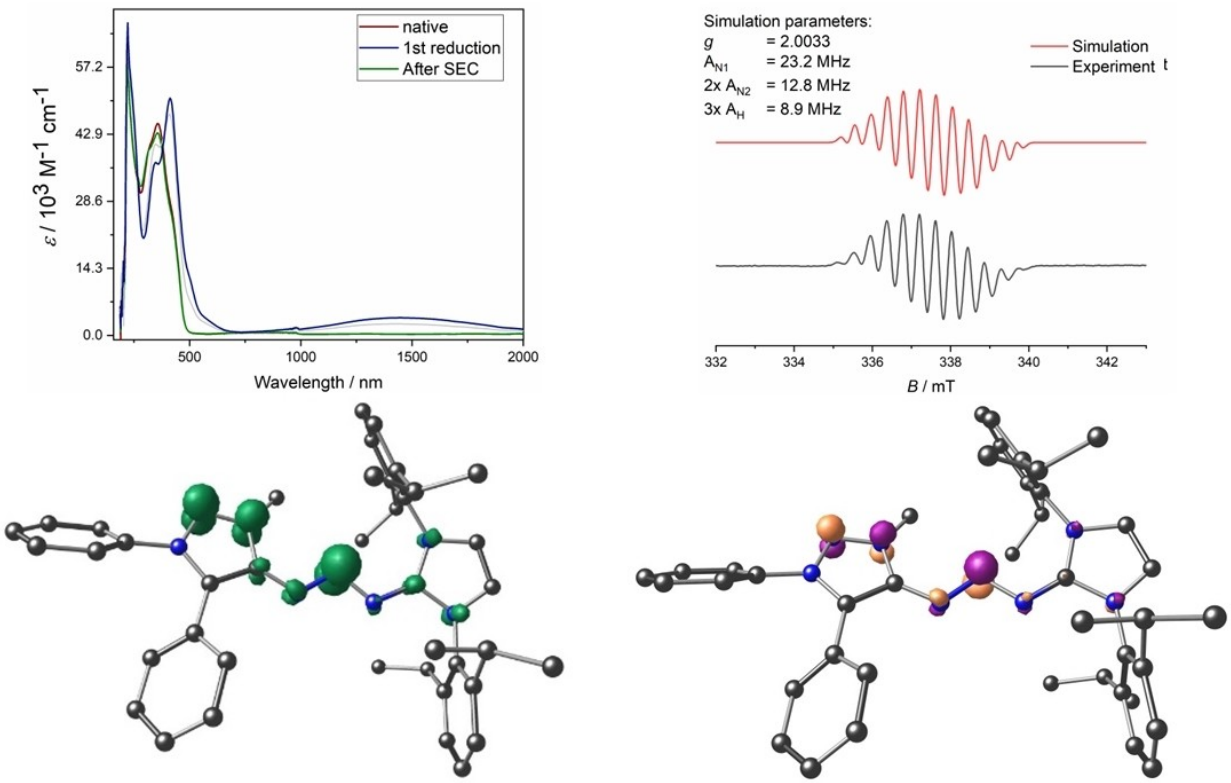

Figure 4. Top left: UV/Vis/NIR spectroelectrochemistry of **MIC-N_3-*i*Pr** measured in DCM/NBu_4PF_6 with a platin electrode. Top right: Experimental EPR spectrum of the in situ electrochemically generated species in DCM/NBu_4PF_6 with a platinum electrode and the simulated spectrum. Bottom left: Spin density calculation of the single reduced **MIC-N_3-*i*Pr** at the UKS PBE D3 def2-SVP def2/J defgrid3 level of theory (isovalue of 0.008). Bottom right: SOMO of the single reduced **MIC-N_3-*i*Pr** (isovalue 0.05).

region disappeared pointing to the potential of these compounds to act as NIR electrochromic dyes. The nature of the radical **[MIC-N_3-*i*Pr]**$^{\cdot}$ was characterised by X-band electron paramagnetic resonance (EPR) spectroscopy. The radical species was generated by electrolysis under potential control using an air-tight three-electrode set-up. The room temperature EPR spectra of the in situ generated species showed an isotropic signal ($g = 2.0033$) with hyperfine splitting due to three ^{14}N and three equivalents ^{1}H nuclei, respectively (Figure 4). The spectrum could be successfully simulated with 2 different sets of ^{14}N nuclei, in accordance with the calculated values (Table S11). The spin population as obtained from the theoretical calculations indicates a major contribution (approximately 30%) from the central nitrogen of the triazene moiety, which translates into a hyperfine coupling constant of 23.2 MHz. With a total contribution of 35%, two nitrogen atoms of the triazolylidene moiety play a crucial role in stabilising the radical by delocalisation of the spin density and therefore also contribute to the hyperfine coupling pattern. The three equivalent hydrogen nuclei can be assigned to the freely rotating methyl group bound to one of the nitrogen nuclei. Interestingly, the terminal nitrogen atoms of the triazene and the NHC moiety displayed no significant contributions to the spin population and hardly contribute to the observed hyperfine coupling. These results are contrary to purely NHC-based triazene radicals in which a fairly symmetrical spin density distribution was observed over both NHC units even for cases in which two different NHCs are bound to the triazene.[12,13] The SOMO of the radical is also predominantly located on the central N-atom of the triazene and the MIC unit, with almost no contribution from the NHC (Figure 4). The above results allow a direct comparison of the properties of a MIC and a NHC in a single molecule. The combination of DFT and EPR shows that the MIC acts as a superior radical stabilizing substituent in comparison to NHC in these compounds which possibly also has consequences for the π-accepting properties of MICs. These results are in accordance with the results of an electrochemically generated triazoline selone radical, where the anionic radical is located on the triazolylidene moiety.[23]

A radical species could also be generated chemically by reacting **MIC-N_3-*i*Pr** with 1.1 equivalents of KC_8 in THF but displayed a spectrum in which the hyperfine coupling to the different nuclei was not as well-resolved as the electrochemically generated species (Figure S34 - S44). This might be due to a high concentration of the radical, which can cause line broadening via intermolecular dipolar interactions and lead to an unfavourable ratio of linewidth to hyperfine coupling constant. These observations show that the concentration has a strong influence on the nature of the EPR signal.

The same SEC measurements were also performed on **MIC-N_3-*i*Mes** and **MIC-N_3-MIC′**. The UV/VIS/NIR spectra showed the

same characteristic features and NIR electrochromism as **MIC-N_3-*I*Pr** (Figure S39). Even though the radical generated for both these cases displayed a similar *g*-value as for [**MIC-N_3-IPr**]$^{\cdot}$, no proper resolution of the hyperfine coupling could be observed for either of these compounds neither for the electrochemically nor for the chemically generated radical species (Figure S44).

Conclusion

In conclusion, we were able to synthesize three different cationic azido-substituted 1,2,3-triazolium salts for the first time, one mono-azide and two compounds with two azide moieties in one molecule. All three building blocks were characterised by NMR spectroscopy, single crystal X-ray diffraction studies, IR-spectroscopy, and mass spectrometry. Additionally, the reactivity of the compounds was investigated via a Staudinger type reactivity under irradiation of light or thermal activation. Treatment with different N-heterocyclic carbenes or a different mesoionic carbene afforded the first examples of MIC/NHC- and MIC/MIC'-based triazenes. We could show that MIC/NHC stabilized triazene radicals can be generated electrochemically and chemically. The nature of the radical was examined with a combination of EPR spectroscopy, cyclic voltammetry, UV/Vis/NIR-spectroelectrochemistry and DFT calculations and showed a major part of the spin density on the triazolylidene moiety. Furthermore, we could show that the triazolylidene unit is crucial for the stabilisation of the radical and acts as a superior electron acceptor compared to the NHC unit. These results, combined with related findings of radical stabilization by MIC units,[23,30,25] open up interesting questions regarding the π-accepting properties of mesoionic carbenes. Additionally, the synthetic route presented by us for generating azide-substituted 1,2,3-triazolium salts should be easily transferable to other 1,2,3-triazolium salts whose synthesis is modular. We thus expect these cationic azido-triazolium synthons to find use in many different fields of synthetic and radical chemistry in the near future.

Experimental Section

Preparation of Compounds: Unless otherwise noted, all reactions were carried out using standard Schlenk-line techniques under an inert atmosphere of argon (Linde, HiQ Argon 5.0, purity $\geq$99.999%). Commercially available chemicals were used without further purification. THF, DCM, acetonitrile and diethyl ether were dried and distilled from sodium/benzophenone. Other solvents were available from MBRAUN MB-SPS-800 solvent system. For the synthesis part, all solvents were degassed by standard techniques prior to use. For NMR spectroscopy, $CDCl_3$ was passed through a small plug basic alumina.^{1}H NMR and $^{13}C\{^1H\}$ NMR spectra were recorded on JEOL ECS 400 spectrometer and JEOL ECZ 400R spectrometer at room temperature. Kinetic NMR spectra were recorded in Fourier transform mode with a Bruker AVANCE 500 spectrometer at 298 K. Chemical shifts are reported in ppm (relative to the TMS signal) with reference to the residual solvent peaks.[31] Multiplets are reported as follows: singlet (s), doublet (d),triplet (t) quartet (q), quintet (quint), and combinations thereof. Mass spectrometry was performed on an Agilent6210 ESI-TOF.

X-ray data were collected on a Bruker D8Venture system at 100(2) K, using graphite-monochromated $Mo_{K\alpha}$ radiation ($\lambda\alpha$ = 0.71073 Å). The strategy for the data collection was evaluated by using the APEX3 software. The data were collected by $\omega+\phi$scan techniques and were scaled and reduced using Saint+ and SADABS software. The structures were solved by intrinsic phasing methods using SHELXT-2014/7. The structure was refined by full matrix least-squares using SHELXL-2014/7, refining on F2. Non-hydrogen atoms were refined anisotropically.[32] The contribution of disordered solvent molecules to the diffraction pattern was subtracted from the observed data by the "SQUEEZE" method as implemented in PLATON.[33]

Deposition Numbers 2173000 (for **1**), 2173022 (for **2**), 2173221 (for **4**), 2173230 (for **6**), 2173023 (for **L1**), 2173223 (for **L2**), 2173679 (for **L3**), 2173279 (for **MIC-N-PPh_3**), and 2173284 (for **MIC-N_3-*I*Pr**) contain the supplementary crystallographic data for this paper. These data are provided free of charge by the joint Cambridge Crystallographic Data Centre and Fachinformationszentrum Karlsruhe Access Structures service.

1,5-Diphenyl-4-chloro-1,2,3-triazole **1** was prepared according to published procedures.[34] 1,1'-Diphenyl-4,4'-bi(1,2,3-triazole) **3** was prepared according to published procedures.[35] **MIC'** was synthesized from the triazolium salt (**7**) according to a literature known procedure.[35]

IR-spectra were recorded on a *Nicolet iS5* spectrometer with an *iD5 ATR* unit from Thermo Fisher Scientific in commercially available DCM. The wavenumbers $\tilde{\nu}$ are given in cm^{-1}.

Cyclic voltammograms were recorded with a PalmSens4 by working in freshly distilled and degassed DCM (99.8% extra dry, Acros Organics) with 0.1 M NBu_4PF_6 (dried, >99.0%, electrochemical grade, Fluka) as the supporting electrolyte. A three-electrode setup was used with glassy carbon as the working electrode, a coiled platinum wire as the counter electrode, and a coiled silver wire as the pseudo reference electrode. The HFc*/HFc^{*+} couple was used as the internal reference.

UV/Vis/NIR spectra were recorded with a J&M TIDAS spectrophotometer. Spectroelectrochemical measurements were carried out in an optically transparent thin-layer electrochemical (OTTLE) cell[36] (CaF_2 windows) with a platin-mesh working electrode (100 mesh woven from 0.064 mm diameter wire; 99.99% (metals basis)), a platinum-mesh counter electrode, and a silver-foil pseudo reference electrode. Anhydrous and degassed DCM ($H_2O \leq 0.005$%, puriss., Sigma Aldrich, distilled from CaH_2) with 0.1 M NBu_4PF_6 as electrolyte was used as the solvent.

EPR spectra at X-band frequency (ca. 9.5 GHz) were obtained with a Magnettech MS-5000 benchtop EPR spectrometer equipped with a rectangular TE 102 cavity. The measurements were carried out in synthetic quartz glass tubes. For EPR spectroelectrochemistry a three-electrode setup was employed using two Teflon coated platinum wires (0.005" bare, 0.008" coated) as working (or a Teflon coated gold wire (0.003" bare, 0.0055" coated) as working electrode) and counter electrode and a Teflon-coated silver wire (0.005" bare, 0.007" coated) as pseudo reference electrode. The EPR spectra have been simulated with MatLab R2012b using Easyspin 5.2.23.[37]

All calculations were performed with the ORCA program package, versions 4.0.1.2 and 4.2.8.[38] The geometries of all species were optimized using the PBE0 functional,[39] the def2-SVP basis sets on all atoms was used.[40] Solvation was taken into account using the using the SMD method together with the CPCM model[41] using DCM as solvent, and dispersion corrections were included using the D3 dispersion correction model.[42] The resolution-of-the identity

(RI) approximation,[43] with matching basis sets,[44] as well as the RIJCOSX approximation (combination of RI and chain-of-spheres algorithm for exchange integrals) were used to reduce the time of calculations. Numerical frequencies calculations were used in order to check that the optimized structures were local minima and to obtain Gibbs free enthalpies. To obtain more reliable energetics single-point calculations were performed using the optimized geometries, the PBE0 functional and def2-TZVP basis sets on all atoms. Low-lying excitation energies were calculated with time-dependent DFT (TD-DFT). For all calculations spin densities were calculated according to the Löwdin population analysis.[45] Broken-symmetry calculations[45,46] were carried out using optimized geometry to evaluate the exchange coupling constants. Plots of spin-densities and optimized geometries were performed using Chemcraft.[47]

4-Chloro-3-methyl-1,5-diphenyl-1,2,3-triazol-3-ium Tetrafluoroborate (2): This ligand was synthesised by following and diversifying a reported procedure.[48] **1** (662 mg, 2.58 mmol, 1 equiv.) and Me_3OBF_4 (957 mg, 6.47 mmol, 3.5 equiv.) were dissolved in DCM (40 mL) and stirred for 3 d. The reaction mixture was poured into diethyl ether (300 mL) and the precipitate was dried in vacuo, affording essentially pure product (857 mg, 2.49 mmol, 93%). ^{1}H NMR (400 MHz, $CDCl_3$): δ = 7.53 (m, 6H, aryl), 7.45 (m, 4H, aryl), 4.24 (s, 3H, N-CH3) ppm. ^{13}C NMR (101 MHz, $CDCl_3$): δ = 139.6, 134.1, 131.9, 131.8, 130.5, 130.0, 129.8, 129.3, 125.9, 121.0, 39.3 ppm. HRMS(ESI): m/z calc. 270.0798 (M^+), found 270.0768 (M^+).

4-Azido-3-methyl-1,5-diphenyl-1,2,3-triazol-3-ium Tetrafluoroborate (L1): **2** (100 mg, 0.279 mmol, 1 equiv.) and sodium azide (90.9 mg; 1.39 mmol; 5 equiv.) were suspended in DCM (10 mL) and stirred for 3 d. The resulting reaction mixture was filtered, and the remaining DCM was evaporated under reduced pressure. The crude product was purified by column chromatography (SiO_2, DCM/MeOH = 20 : 1). The product was obtained as a white solid (72 mg, 0.197 mmol, 70%). ^{1}H NMR (400 MHz, $CDCl_3$): δ = 7.54 (m, 6H, aryl), 7.46 (m, 4H, aryl), 4.23 (s, 3H, N-CH_3) ppm. ^{13}C NMR (101 MHz, $CDCl_3$): δ = 140.4, 134.2, 131.8, 131.7, 130.4, 130.2, 129.7, 129.2, 126.1, 121.4, 37.7.ppm. HRMS(ESI): m/z calc. 277.1202 (M^+), found 277.1211 (M^+).

5,5′-Dichloro-1,1′-diphenyl-4,4′-bi(1,2,3-triazole) (4): This ligand was synthesised by following and diversify a reported procedure.[49] **3** (500 mg, 1.73 mmol, 1 equiv.) was suspended in THF (20 mL). After addition of KO^{t}Bu (388 mg, 3.46 mmol, 2.1 equiv.) the solution turns orange with white precipitate. After 10 min stirring and cooling down to 0 °C, the hexachloroethane (820 mg, 3.465 mmol, 2.1 equiv.) was added. The mixture was stirred for 12 h, while the colour changed to bright yellow. The crude product was purified by column chromatography (SiO_2, DCM/Acetone = 100 : 1). The product was obtained as a white solid (438 mg, 1.22 mmol, 71%). ^{1}H NMR (400 MHz, $(CD_3)_2CO$)): δ = 7.79 (m, 4H, aryl), 7.72 (m, 6H, aryl) ppm. ^{13}C NMR (101 MHz, $(CD_3)_2CO$) δ = 135.9, 134.9, 131.4, 130.6, 126.4 ppm. HRMS(ESI): m/z calc. 379.0236 ($M+Na^+$), found 379.0240 ($M+Na^+$).

5,5′-Dichloro-3,3′-dimethyl-1,1′-diphenyl-[4,4′-bi(1,2,3-triazol-3,3′-diium)] Tetrafluoroborate (5): This ligand was synthesised by following and diversify a reported procedure.[48] **4** (431 mg, 1.22 mmol, 1 equiv.) and Me_3OBF_4 (543 mg; 3.67 mmol; 3 equiv.) were dissolved in DCM (30 mL) and stirred for 3 d. The reaction mixture was poured into diethyl ether (300 mL) and the precipitate was dried in vacuo, affording essentially pure product (608 mg, 1.08 mmol, 89%). ^{1}H NMR (400 MHz, DMSO-d^6): δ = 7.91 (m, 10H, aryl), 4.64 (s, 6H, N-CH_3) ppm.^{13}C NMR (101 MHz, DMSO-d^6): δ = 135.8, 133.3, 132.0, 130.6, 125.8, 122.7, 41.1 ppm. Anal. Calcd. for $C_{18}H_{15}N_6F_8Cl_2B_2$: C, 38.62; H, 2.70; N, 15.01. Found: C, 38.55; H, 2.861; N, 15.00.

5,5′-Diazido-3,3′-dimethyl-1,1′-diphenyl-[4,4′-bi(1,2,3-triazole)]-3,3′-diium Tetrafluoroborate (L2): **5** (80.0 mg, 0.142 mmol, 1 equiv.) and sodium azide (92 mg; 1.42 mmol; 10 equiv.) were suspended in DCM (20 mL) and stirred for 3 d. The resulting reaction mixture was filtered, and the remaining DCM was evaporated under reduced pressure. The crude product was purified by column chromatography (SiO_2, DCM/MeOH = 20 : 1). The product was obtained as a white solid (59.5 mg, 0.103 mmol, 73%). ^{1}H NMR (400 MHz, $(CD_3)_2CO$)): δ = 8.06 (m, 4H, aryl), 7.89 (m, 6H, aryl), 4.70 (s, 6H, N-CH_3) ppm. ^{13}C NMR (126 MHz, (DMSO-d^6)): δ = 140.9, 133.2, 131.6, 130.5, 125.7, 114.1, 40.9 ppm. HRMS(ESI): m/z calc. 277.1202 (M^+), found 277.1211 (M^+).

Bis(4-chloro-1,5-diphenyl-1,2,3-triazol-3-yl)methane Ditriflate (6): This ligand was synthesised by following and diversify a reported procedure.[48] Silver triflate (356 mg, 1.38 mmol, 2.2 equiv.) was suspended in hexane (10 mL). After adding of freshly distilled diiodomethane (0.081 mL, 0.63 mmol, 1 equiv.), the mixture was heated to 70 °C and stirred for 4 h under exclusion of light. The corresponding suspension with the participating silver iodide was filtered over a plug of Celite@ and washed with hexane (5 mL). The filtrate was added dropwise to **1** (402 mg, 1.56 mmol, 2.5 equiv.) in toluene (10 mL). The resulting mixture was heated to refluxed overnight. After cooling down to room temperature, the solution was diluted in diethyl ether (500 mL). The resulting colourless precipitate was collected by filtration and washed with diethyl ether (50-100 mL), to obtain the product as a colourless solid (254 mg, 0.309 mmol, 49%). ^{1}H NMR (400 MHz, $(CDCl_3)$): δ = 7.40 (m, 16H, aryl-H), 7.81 (m, 4H, aryl-H), 7.32 (s, 2H, methylene-H), 7.30 (m, 2H, aryl-H), 7.27 (m, 2H, aryl-H) ppm. ^{13}C NMR (101 MHz, $(CDCl_3)$): δ = 140.7, 133.4, 132.3, 132.1, 131.3, 130.4, 129.7, 129.0, 126.4, 120.7, 60.3 ppm. HRMS(ESI): m/z calc 262.0636 (M^{2+}), found 262.0666 (M^{2+}).

Bis(4-azido-1,5-diphenyl-1,2,3-triazol-3-yl)methane Ditriflate (L3): **6** (41.1 mg, 0.05 mmol, 1 equiv.) and sodium azide (33.0 mg; 0.50 mmol; 10 equiv.) were suspended in DCM (3 mL) and stirred for 3 d. The resulting reaction mixture was filtered, and the remaining DCM was dropped in stirred Et_2O (200 mL). The white precipitate was filtrated, washed with Et_2O and dried. The product was obtained as a white solid (33.8 mg, 0.0405 mmol, 81%). ^{1}H NMR (400 MHz, $(CDCl_3)$): δ = 7.40 (m, 16H, aryl-H), 7.81 (m, 4H, aryl-H), 7.32 (s, 2H, methylene-H), 7.30 (m, 2H, aryl-H), 7.27 (m, 2H, aryl-H) ppm. ^{13}C NMR (126 MHz, $(CDCl_3)$): δ = 138.5, 134.2, 134.0, 132.0, 131.9, 131.4, 129.6, 129.0, 126.4, 121.8, 120.3, 119.3, 58.46 ppm. HRMS(ESI): m/z calc: 687.1665 (M-OTf)$^+$, found: 687.1669 (M-OTf)$^+$.

MIC-N-PPh_3

Procedure I: **L1** (36.4 mg, 0.1 mmol, 1 equiv.) and PPh_3 (27.0 mg, 0.103 mmol, 1.03 equiv.) were suspended in THF. The suspension was irradiated with light (256 nm) for 1 h, while the solution changed the colour from colourless to bright yellow. The solvent was evaporated and the remaining solid was washed with toluene. The product was obtained after recrystallization from DCM and hexane as a white solid (55.0 mg, 0.92 mmol, 92%).

Procedure II: **L1** (36.4 mg, 0.1 mmol, 1 equiv.) and PPh_3 (27.0 mg, 0.103 mmol, 1.03 equiv.) were suspended in toluene. The suspension was heated for 1 h at 70 °C, while the solution changed the colour from colourless to bright yellow. The solvent was evaporated and the remaining solid was washed with toluene. The product was obtained after recrystallization from DCM and hexane as a white solid (55.0 mg, 0.92 mmol, 92%).

^{1}H NMR (250 MHz, $(CD_3)_2CO$)): δ = 7.58 (20H, m, aryl), 7.24 (m, 2H, aryl), 7.06 (m, 2H, aryl), 6.90 (m, 2H, aryl), 4.15 (s. 3H, N-CH_3) ppm.

^{13}C NMR (101 MHz, ($CDCl_3$)): δ = 206.1, 136.3, 133.8, 133.8, 133.1, 133.07, 132.21 132.0, 131.0, 130.4, 130.1, 130.0, 129.8, 129.5, 128.9, 126.6, 125.2, 35.8. ppm. ^{31}P NMR (101 MHz, ($CD_3)_2CO$)): δ = 10.98 ppm. HRMS(ESI): m/z calc 511.2052 (M^+), found 511.2048 (M^+).

MIC-N_3-*I*Pr: In an argon glovebox, **L1** (23.0 mg, 0.063 mmol, 1 equiv.) and 1,3-bis-(2,6-diisopropylphenyl)-1,3-dihydro-2H-imidazol-2-yliden (37 mg, 0.098 mmol, 1.5 equiv.) were suspended in THF (5 mL). The mixture was stirred for 18 h under the exclusion of light. The resulting yellow solution was filtered, and the solvent was evaporated. The yellow solid was purified in two steps: First, a column chromatography (SiO_2, DCM/MeOH = 10 : 1) was performed, with subsequently recrystallization from ethyl acetate und pentane at −20 °C. The product was obtained as a yellow solid (17.6 mg, 0.023 mmol, 37 %). ^{1}H NMR (250 MHz, (CD_2Cl_2)): δ = 7.56 (m, 5H, aryl), 7.34 (m, 9H, aryl), 7.07 (m, 2H, aryl), 7.01 (s, 2H, NHC-backbone), 3.11 (s, 3H, N-CH3), 2.70 (sept, 4H, CH-($CH_3)_2$), 1.27 (d, 12H, *J* = 6.75 Hz, CH_3-Ch), 1.14 (d, 12H, *J* = 6.71 Hz, CH_3-Ch) ppm. ^{13}C NMR (376 MHz, (CD_2Cl_2)): δ = 207.2, 151.0, 146.9, 146.1, 145.6, 134.7, 133.2, 132.82 132.7, 132.5, 131.5, 131.5, 130.7, 130.4, 129.5, 126.7, 125.6, 125.3, 125.2, 122.9, 121.2, 38.5, 29.7, 23.9, 23.48 ppm. HRMS(ESI): m/z calc 667.4231 (M^+), found 667.4196 (M^+).

MIC-N_3-*I*Mes: In an argon glovebox, **L1** (34.6 mg, 0.095 mmol, 1 equiv.) and 1,3-bis-(2,4,6-trimethylphenyl)-1,3-dihydro-2H-imidazol-2-ylide (43.7 mg, 0.143 mmol, 1.5 equiv.) were suspended in THF (5 mL). The mixture was stirred for 18 h under the exclusion of light. The resulting yellow solution was filtered, and the solvent was evaporated. The yellow solid was purified in two steps: First, a column chromatography (SiO_2, DCM/MeOH = 10 : 1) was performed, with subsequently recrystallization from ethyl acetate und pentane at −20 °C. The product was obtained as a yellow solid (20.3 mg, 0.0304 mmol, 32 %). ^{1}H NMR (250 MHz, (CD_2Cl_2)): δ = 7.43 (m, 10H, aryl), 7.09 (m, 2H, NHC-backbone), 6.93 (s, 4H, Mes), 3.54 (s, 3H, N-CH_3), 2.28 (s, 6H, Mes(CH_3)), 2.21 (s, 12H, Mes(CH_3)) ppm. ^{13}C NMR (126 MHz, (CD_2Cl_2)): δ = 161.8, 139.3, 135.8, 134.4, 133.9, 132.4, 131.5, 130.6, 130.3, 129.9, 129.5, 125.4, 122.6, 48.7, 38.7, 17.96 ppm. HRMS(ESI): m/z calc 581.3136 (M^+), found 581.3127 (M^+).

MIC-N_3-MIC': Under argon atmosphere, **L1** (64.8 mg, 0.178 mmol, 1.5 equiv.) was suspended in THF (3 mL). In a second flask, **MIC(Mes)** (48.3 mg, 0.118 mmol. 1 equiv.) was suspended in THF (3 mL) and KHMDS (30.7 mg, 0.154 mmol, 1.3 equiv.) was added and stirred for 30 min. The solution was filtered over a syringe filter and transferred to the first flask. The combined solutions were stirred for 16 h under the exclusion of light. The resulting yellow solution was filtered, and the solvent was evaporated. The yellow solid was purified in two steps: First, a column chromatography (SiO_2, DCM/MeOH = 10 : 1) was performed, with subsequently recrystallization from ethyl acetate und pentane at −20 °C. The product was obtained as a yellow solid (15.0 mg, 0.028 mmol, 18 %). ^{1}H NMR (250 MHz, (CD_2Cl_2)): δ = 7.52 (m, 4H, aryl), 7.32 (m, 4H, aryl), 7.20 (m, 2H, aryl), 7.12 (s, 4H, aryl), 3.91 (s, 3H, N-CH_3), 3.19 (s, 3H, N-CH_3), 2.41 (s, 6H, Mesityl), 2.10 (s, 12H, mesityl) ppm. ^{13}C NMR (101 MHz, (CD_2Cl_2)): δ = 151.0, 147.4, 142.5, 139.0, 135.4, 134.8, 132.0, 130.9, 130.5, 130.4, 129.9, 129.7, 129.3, 125.3, 123.6, 121.3, 77.94, 39.3, 38.4, 31.9, 23.0, 22.7, 21.4, 20.2, 17.6, 14.2. ppm. HRMS(ESI): m/z calc 596.3243 (M^+), found 596.3250 (M^+).

Acknowledgements

We would like to acknowledge the assistance of the Core Facility BioSupraMol supported by the DFG. Arijit Singha Hazari kindly acknowledges funding from the innovation programme under the Marie Skłodowska-Curie grant agreement No. 894082. The authors acknowledge support by the state of Baden-Württemberg through bwHPC and the German Research Foundation (DFG) through grant no INST 40/575-1 FUGG (JUSTUS 2 cluster). Open Access funding enabled and organized by Projekt DEAL.

Conflict of Interests

The authors declare no conflict of interest.

Data Availability Statement

The data that support the findings of this study are available in the supplementary material of this article.

Keywords: cationic azides · mesoionic carbene · radicals · spectroelectrochemistry · triazenes

[1] J. P. Griess, *Phil. Trans. R. Soc.* **1864**, *154*, 667–731.
[2] S. Bräse, C. Gil, K. Knepper, V. Zimmermann, *Angew. Chem. Int. Ed.* **2005**, *44*, 5188–5240.
[3] a) L. Horner, A. Christmann, *Angew. Chem. Int. Ed.* **1963**, *2*, 599–608; b) M.-L. Tsao, M. S. Platz, *J. Am. Chem. Soc.* **2003**, *125*, 12014–12025.
[4] a) P. Magnus, K. S. Matthews, V. Lynch, *Org. Lett.* **2003**, *5*, 2181–2184; b) J. H. Boyer, J. Hamer, *J. Am. Chem. Soc.* **1955**, *77*, 951–954.
[5] H. Staudinger, J. Meyer, *Helv. Chim. Acta* **1919**, *2*, 635–646.
[6] B. Chen, A. K. Mapp, *J. Am. Chem. Soc.* **2004**, *126*, 5364–5365.
[7] a) R. Huisgen, R. Knorr, L. Möbius, G. Szeimies, *Chem. Ber.* **1965**, *98*, 4014–4021; b) R. Huisgen, H. Gotthardt, H. O. Bayer, F. C. Schaefer, *Angew. Chem. Int. Ed.* **1964**, *3*, 136–137.
[8] a) M. N. Hopkinson, C. Richter, M. Schedler, F. Glorius, *Nature* **2014**, *510*, 485–496; b) Y. Kim, E. Lee, *Chem. Eur. J.* **2018**, *24*, 19110–19121.
[9] a) H. Balli, R. Maul, *Helv. Chim. Acta* **1976**, *59*, 148–155; b) H. Xue, Y. Gao, B. Twamley, J. M. Shreeve, *Chem. Mater.* **2005**, *17*, 1, 191–198; c) G. Laus, A. Schwärzler, P. Schuster, G. Bentivoglio, M. Hummel, K. Wurst, V. Kahlenberg, T. Lörting, J. Schütz, P. Peringer, G. Bonn, G. Nauer, H. Schottenberger, *Z. Naturforsch.* **2007**, *62b*, 295–308; d) M. Kitamura, *Org. Synth.* **2015**, *92*, 171–181.
[10] G. Laus, M. E. Kostner, V. Kahlenberg, H. Schottenberger, *Z. Naturforsch. B* **2016**, *71*, 997–1003.
[11] a) D. M. Khramov, C. W. Bielawski, *J. Org. Chem.* **2007**, *72*, 9407–9417; b) A. G. M. Barrett, M. R. Crimmin, M. S. Hill, P. B. Hitchcock, G. Kociok-Köhn, P. A. Procopiou, *Inorg. Chem.* **2008**, *47*, 7366–7376; c) R. Naef, H. Balli, *Helv. Chim. Acta* **1978**, *61*, 2958–2973; d) S. Patil, A. Bugarin, *Acta Crystallogr. Sect. E* **2014**, *70*, 224–227; e) A. G. Tennyson, E. J. Moorhead, B. L. Madison, J. A. V. Er, V. M. Lynch, C. W. Bielawski, *Eur. J. Org. Chem.* **2010**, *2010*, 6277–6282; f) D. Winkelhaus, M. H. Holthausen, R. Dobrovetsky, D. W. Stephan, *Chem. Sci.* **2015**, *6*, 6367–6372; g) S. Patil, A. Bugarin, *Eur. J. Org. Chem.* **2016**, 860–870.
[12] J. Back, J. Park, Y. Kim, H. Kang, Y. Kim, M. J. Park, K. Kim, E. Lee, *J. Am. Chem. Soc.* **2017**, *139*, 15300–15303.
[13] J. Back, G. Kwon, J. E. Byeon, H. Song, K. Kang, E. Lee, *ACS Appl. Mater. Interfaces* **2020**, *12*, 37338–37345.
[14] S. Patil, K. White, A. Bugarin, *Tetrahedron Lett.* **2014**, *55*, 4826–4829.
[15] G. Laus, V. Kahlenberg, H. Schottenberger, *Crystals* **2016**, *6*, 20–29.
[16] M. Kitamura, S. Kato, M. Yano, N. Tashiro, Y. Shiratake, M. Sando, T. Okauchi, *Org. Biomol. Chem.* **2014**, *12*, 4397–4406.
[17] a) O. Back, B. Donnadieu, M. von Hopffgarten, S. Klein, R. Tonner, G. Frenking, G. Bertrand, *Chem. Sci.* **2011**, *2*, 858–861; b) M. Soleilhavoup, G. Bertrand, *Acc. Chem. Res.* **2015**, *48*, 256–266; c) L. Y. M. Eymann, A. G. Tskhovrebov, A. Sienkiewicz, J. L. Bila, I. Živković, H. M. Rønnow, M. D. Wodrich, L. Vannay, C. Corminboeuf, P. Pattison, E. Solari, R. Scopelliti, K. Severin, *J. Am. Chem. Soc.* **2016**, *138*, 15126–15129; d) C. D. Martin, M. Soleilhavoup, G. Bertrand, *Chem. Sci.* **2013**, *4*, 3020–3030; e) D. Mandal,

R. Dolai, N. Chrysochos, P. Kalita, R. Kumar, D. Dhara, A. Maiti, R. S. Narayanan, G. Rajaraman, C. Schulzke, V. Chandrasekhar, A. Jana, *Org. Lett.* **2017**, *19*, 5605–5608; f) M. Melaimi, R. Jazzar, M. Soleilhavoup, G. Bertrand, *Angew. Chem. Int. Ed.* **2017**, *56*, 10046–10068; g) J. Messelberger, A. Grünwald, P. Pinter, M. M. Hansmann, D. Munz, *Chem. Sci.* **2018**, *9*, 6107–6117; h) M. M. Hansmann, M. Melaimi, G. Bertrand, *J. Am. Chem. Soc.* **2018**, *140*, 2206–2213; i) R. S. Ghadwal, *Synlett* **2019**, *30*, 1765–1775; j) Y. K. Loh, P. Vasko, C. McManus, A. Heilmann, W. K. Myers, S. Aldridge, *Nat. Commun.* **2021**, *12*, 7052–7059; k) M. K. Nayak, P. Sarkar, B. J. Elvers, S. Mehta, F. Zhang, N. Chrysochos, I. Krummenacher, T. Vijayakanth, R. S. Narayanan, R. Dolai, B. Roy, V. Malik, H. Rawat, A. Mondal, R. Boomishankar, S. K. Pati, H. Braunschweig, C. Schulzke, P Ravat, A. Jana, *Chem. Sci.* **2022**, *13*, 12533–12539; l) H. Song, E. Pietrasiak, E. Lee, *Acc. Chem. Res.* **2022**, *55*, 16, 2213–2223.
[18] Y. Liu, P. Varava, A. Fabrizio, L. Y. M. Eymann, A. G. Tskhovrebov, O. M. Planes, E. Solari, F. Fadaei-Tirani, R. Scopelliti, A. Sienkiewicz, C. Corminboef, K. Severin, *Chem. Sci.* **2019**, *10*, 5719–5724.
[19] K. Breitwieser, H. Bahmann, R. Weiss, D. Munz, *Angew. Chem. Int. Ed.* **2022**, *61*, e202206390.
[20] R. Maity, B. Sarkar, *JACS Au* **2022**, *2*, 22–57.
[21] D. Schweinfurth, L. Hettmanczyk, L. Suntrup, B. Sarkar, *Z. Anorg. Allg. Chem.* **2017**, *643*, 554–584.
[22] L. Y. M. Eymann, R. Scopelliti, F. F. Tirani, K. Severin, *Chem. Eur. J.* **2018**, *24*, 7957–7963.
[23] J. Beerhues, M. Neubrand, S. Sobottka, N. I. Neuman, H. Aberhan, S. Chandra, B. Sarkar, *Chem. Eur. J.* **2021**, *27*, 6557–6568.
[24] T. Bens, P. Boden, P. Di Martino-Fumo, J. Beerhues, U. Albold, S. Sobottka, N. I. Neuman, M. Gerhards, B. Sarkar, *Inorg. Chem.* **2020**, *59*, 15504–15513.
[25] W. Liu, A. Vianna, Z. Zhang, S. Huang, L. Huang, M. Melaimi, G. Bertrand, X. Yan, *Chem. Catalysis* **2021**, *1*, 196–206.
[26] a) S. Vanicek, M. Podewitz, J. Stubbe, D. Schulze, H. Kopacka, K. Wurst, T. Müller, P. Lippmann, S. Haslinger, H. Schottenberger, K. L. Liedel, I. Otto, B. Sarkar, B. Billstein, *Chem. Eur. J.* **2018**, *24*, 3742–3753; b) S. Vanicek, J. Beerhues, T. Bens, V. Levchenko, K. Wurst, B. Bildstein, M. Tilset, B. Sarkar, *Organometallics* **2019**, *38*, 4383–4386.
[27] M. Kitamura, A. Ishikawa, T. Okauchi, *Tetrahedron Lett.* **2016**, *57*, 1794–1797.
[28] S. Haslinger, G. Laus, V. Kahlenberg, K. Wurst, T. Bechtold, S. Vergeiner, H. Schottenberger, *Crystals* **2016**, *6*, 40–52.
[29] F. Stein, M. Kirsch, J. Beerhues, U. Albold, B. Sarkar, *Eur. J. Inorg. Chem.* **2021**, *2021*, 2417–2424.
[30] J. Stubbe, S. Suhr, J. Beerhues, M. Nößler, B. Sarkar, *Chem. Sci.* **2021**, *12*, 3170–3178.
[31] G. R. Fulmer, A. J. M. Miller, N. H. Sherden, H. E. Gottlieb, A. Nudelman, B. M. Stoltz, J. E. Bercaw, K. I. Goldberg, *Organometallics* **2010**, *29*, 2176–2179.
[32] a) *APEX3*, Bruker AXS Inc., Madison, Wisconsin, USA, **2015**; b) G. M. Sheldrick, *SADABS Ver. 2008/1, Program for Empirical Absorption Correction*, University of Göttingen, Germany, **2008**; c) *SAINT+, Data Integration Engine, Version 8.27b* ©, Bruker AXS Inc., Madison, Wisconsin, USA, 1997–2012; d) G. M. Sheldrick, *SHELXL Version 2014/7, Program for Chrystal Structure Solution and Refinement*, University of Göttingen, Germany, **2014**; e) C. B. Hübschle, G. M. Sheldrick, B. Dittrich, *J. Appl. Crystallogr.* **2011**, *44*, 1281–1284; f) G. M. Sheldrick, *Acta Crystallogr. Sect. A* **2008**, *64*, 112–122; g) G. M. Sheldrick, *Acta Crystallogr. Sect. C* **2015**, *71*, 3.17; h) A. L. Spek, *Acta Crystallogr. Sect. C* **2015**, *71*, 9–18; i) A. L. Spek, *Acta Crystallogr.* **2009**, *D65*, 148–155; j) A. L. Spek, *J. Appl. Crystallogr.* **2003**, *36*, 7–13.
[33] A. L. Spek, *PLATON, A multipurpose Crystallographic Tool*, Utrecht, the Netherlands, **1998**.
[34] I. V. Karsakova, A. Y. Smirnov, M. S. Baranov, *Chem. Heterocycl. Compd.* **2018**, *54*, 755–757.
[35] J. T. Fletcher, B. J. Bumgarner, N. D. Engels, D. A. Skoglund, *Organometallics* **2008**, *27*, 5430–5433.
[36] M. Krejčik, M. Daněk, F. Hartl, *J. Electroanal. Chem. Interfacial Electrochem.* **1991**, *317*, 179–187.
[37] S. Stoll, A. Schweiger, *J. Magn. Reson.* **2006**, *178*, 42–55.
[38] F. Neese, *WIREs Comput. Mol. Sci.* **2018**, *8*, 33–39.
[39] C. Adamo, V. Barone, *J. Chem. Phys.* **1999**, *110*, 6158–6170.
[40] F. Weigend, R. Ahlrichs, *Phys. Chem. Chem. Phys.* **2005**, *7*, 3297–3305.
[41] V. Barone, M. Cossi, *J. Phys. Chem. A* **1998**, *102*, 1995–2001.
[42] a) S. Grimme, *J. Comput. Chem.* **2006**, *27*, 1787–1799; b) S. Grimme, *J. Comput. Chem.* **2004**, *25*, 1463–1473; c) S. Grimme, J. Antony, S. Ehrlich, H. Krieg, *J. Chem. Phys.* **2010**, *132*, 154104–154122; d) S. Grimme, S. Ehrlich, L. Goerigk, *J. Comput. Chem.* **2011**, *32*, 1456–1465.
[43] a) P. Seth, P. L. Ríos, R. J. Needs, *J. Chem. Phys.* **2011**, *134*, 84105–84114; b) F. Neese, G. Olbrich, *Chem. Phys. Lett.* **2002**, *362*, 170–178; c) R. Izsák, F. Neese, *J. Chem. Phys.* **2011**, *135*, 144105–144117; d) J. L. Whitten, *J. Chem. Phys.* **1973**, *58*, 4496–4502; e) O. Vahtras, J. Almlöf, M. W. Feyereisen, *Chem. Phys. Lett.* **1993**, *213*, 514–518; f) F. Neese, F. Wennmohs, A. Hansen, *J. Chem. Phys.* **2009**, *130*, 114108–114126; g) F. Neese, *J. Comput. Chem.* **2003**, *24*, 1740–1747.
[44] a) K. Eichkorn, O. Treutler, H. Öhm, M. Häser, R. Ahlrichs, *Chem. Phys. Lett.* **1995**, *240*, 283–290; b) K. Eichkorn, F. Weigend, O. Treutler, R. Ahlrichs, *Theor. Chem. Acc.* **1997**, *97*, 119–124; c) F. Weigend, *Phys. Chem. Chem. Phys.* **2006**, *8*, 1057–1065.
[45] P.-O. Löwdin, *J. Chem. Phys.* **1950**, *18*, 365–377.
[46] a) D. Doehnert, J. Koutecky, *J. Am. Chem. Soc.* **1980**, *102*, 1789–1796; b) J. Gräfenstein, E. Kraka, M. Filatov, D. Cremer, *Int. J. Mol. Sci.* **2002**, *3*, 360–394; c) F. Neese, *J. Phys. Chem. Solids* **2004**, *65*, 781–785; d) K. Yamaguchi, *Chem. Phys. Lett.* **1975**, *33*, 330–335.
[47] Chemcraft – graphical software for visualization of quantum chemistry computations (Chemcraft).
[48] S. Hohloch, L. Suntrup, B. Sarkar, *Organometallics* **2013**, *32*, 7376–7385.
[49] J. Back, J. Park, Y. Kim, H. Kang, Y. Kim, M. J. Park, K. Kim, E. Lee, *J. Am. Chem. Soc.* **2017**, *139*, 15300–15303.

Manuscript received: March 9, 2023
Accepted manuscript online: April 12, 2023
Version of record online: May 12, 2023